



Synchronous analysis of brain regions based on multi-scale permutation transfer entropy



Yunyuan Gao^{a,**}, Huixu Su^a, Rihui Li^b, Yingchun Zhang^{b,*}

^a Intelligent Control & Robotics Institute, College of Automation, Hangzhou Dianzi University, Hangzhou, China

^b Department of Biomedical Engineering, University of Houston, Houston, TX, USA

ARTICLE INFO

Keywords:

Multi-scale permutation transfer entropy
Synchronous relationship
Electroencephalography

ABSTRACT

The coupling of electroencephalographic (EEG) signals reflects the interaction between brain regions, which is of great importance for the assessment of motor function in post-stroke patients. In this study, the measurement of multi-scale permutation transfer entropy (MPTE) was presented and employed to characterize the coupling between the EEG signals measured from the bilateral motor and sensory areas. Post-stroke patients ($n = 5$) and healthy volunteers ($n = 6$) were recruited and participated in a hand grip task with different levels of contraction. MPTE values were computed and analyzed across various frequency bands for all subjects. Results showed that, for healthy controls, the coupling between motor and sensory areas was bi-directional and tended to be strongest in beta band. In particular, greater beta-band MPTE was found in the dominant hand and coupling strength decreased as contraction strength increased. Additionally, coupling between the motor and sensory areas of stroke patients exhibited weaker beta-band MPTE than that of healthy controls. Findings suggest that MPTE is able to quantitatively characterize the coupling properties between multiple brain regions, providing a promising approach to study the underlying mechanisms of functional motor recovery.

1. Introduction

Electroencephalogram (EEG) is a non-invasive brain imaging technique that uses an array of scalp electrodes to measure the voltage fluctuations induced by the mass activity of neurons. These voltage signals hold great information about functional activity within the brain. This is particularly true for motor tasks, where relevant brain regions tend to synchronize with each other, establishing orderly brain function [1]. For example, previous study has shown synchronous relationships between the somatosensory and motor areas of monkeys engaged in a motor task [2]. Coupling between relevant brain areas has also been observed in humans during motion and cognition [3,4]. Exploring regional coupling therefore provides an avenue through which the mechanisms of motor function can be studied, and a theoretical basis for the rehabilitation of stroke patients with motor dysfunction.

At present, both non-linear and linear methods have been developed to assess the coupling of cortical EEG signals [5,6], although recent evidence has suggested that brain activity is nonlinear, raising questions as to the validity of linear approaches. This has led to an increase in the use of nonlinear coupling analysis methods, including phase synchronization [7], mutual information [8], coherence analysis

[9,10], to assess the interaction between brain regions. In particular, permutation mutual information, defined as the arrangement pattern of the mutual information within signals, is one of the most effective methods for investigating the coupling between specific brain regions. Previous studies have employed this approach, including single and multi-scale permutation entropy, to analyze the coupling properties of EEG signals in healthy subjects as well as various patient groups, providing evidence that permutation mutual information can be used to enhance the calculation of mutual information of EEG signals [11–13].

To further analyze the directional relationship between physiological signals, measures of causality, including Granger causality and transfer entropy (TE), have been employed to assess the directional coupling between signals [14–16]. Unfortunately, Granger causality is a linear method that cannot effectively characterize the nonlinear and multi-scale properties of physiological signals [17,18]. On the contrary, the TE is a nonlinear directed information transfer method that evaluates the bivariate information transfer between coupled time series and is capable of model-free analyses for physiological systems. TE is subject to some limitations, however, as it requires a large amount of continuous data and is highly sensitive to noise. Several enhanced forms of TE have therefore been developed to satisfy the specific needs

* Corresponding author. Department of Biomedical Engineering University of Houston, Houston, TX, 77004, USA.

** Corresponding author.

E-mail address: y Zhang (Y. Zhang).

of different applications. For instance, symbolic transfer entropy (STE) makes use of a symbolization technique (i.e. permutation) and transfer entropy to overcome the requirement for a long data segment; while multi-scale transfer entropy (MTE) was designed to be capable of characterizing physiological signals at multiple scales [19–21]. Unfortunately, both STE and MTE have a limited ability to analyze the coupling relationships between signals. STE focuses on single-scale analysis and thereby fails to offer a comprehensive coupling profile of signals. MTE, similar to the traditional calculation of mutual information, requires a large amount of data to accurately estimate the probability density functions that are necessary for the calculation of transfer entropy, making it difficult to precisely capture coupling properties of EEG signals [22,23]. Consequently, there is a clear need to develop novel techniques that can address these challenges by identifying coupling across multiple scales using a minimal amount of data.

Taking the advantage of the individual properties of STE and MTE, a novel method called multi-scale permutation transfer entropy (MPTE) has been developed to analyze the coupling properties between the motor and sensory areas of both healthy volunteers and stroke patients during a three-level hand grip task. In particular, coupling strength was assessed based on the EEG signals measured from the bilateral motor cortices at different frequency bands and different scales. It is hypothesized that the motor impairment caused by stroke would alter the direction and strength of coupling between brain areas, providing a basis for the functional evaluation of motor rehabilitation.

2. Materials and methods

2.1. Participants

Eleven right-handed male subjects were recruited in this study, including a control group (n = 6, age: 24.7 ± 1.21 years) and a patient group (n = 5, age: 48 ± 2.24 years). All stroke locations were lateralized to the left hemisphere, causing motor dysfunction on the right side of the body. Subject demographic information is summarized in Table 1. The study protocol was approved by the Institutional Review Board of Guangdong Provincial Work-Injury Rehabilitation Hospital. Prior to the experiment, all the subjects were fully informed of the details of the experiment and signed the informed consent form.

2.2. Experimental paradigm

All experiments were performed in an isolated room to reduce any environmental disturbance. Subjects were seated on a wooden chair and held a spring grip meter (EH101, Lynx Mall, China). The paradigm used in this study included three levels of hand grip tasks (5 kg, 10 kg, and 20 kg), as illustrated in Fig. 1. Each task started with a 20 s resting condition that was followed by a motor task, wherein subjects were asked to perform a hand grip task for 5 s in accordance with instructions displayed on a screen 1-m in front of their eyes. Subjects were allowed to rest for 20 s in between each trial. Each motor task was repeated five times, and all subjects performed each motor task using both their left and right hands. After each motor task was completed, the subjects rested for 20 min to prevent muscle fatigue. It should be noted that, as stroke patients were unable to perform the grip task at the 10 kg and 20 kg levels, only the 5 kg task and maximum voluntary contraction

(MVC) measurements were collected for the patient group.

2.3. Data collection

A 32-channel EEG acquisition system (Brain Products GmbH, Germany) was utilized to collect EEG signals (Fig. 2a). EEG electrodes were placed on the scalp according to the international 10–20 standard system, as shown in Fig. 2b. Before the electrodes were placed, the scalp was cleaned and the sampling frequency was set to 1000Hz.

2.4. EEG preprocessing

In this study, in order to assess the coupling between the motor and sensory areas of the brain during the motor task, EEG signals from the C3, C4, CP5, and CP6 channels were selected for analysis.

As EEG signals are susceptible to noise and power frequency interference, the collected EEG data were preprocessed using BrainVision Analyzer 2.0 software (Brain Products, Germany) to remove powerline interference, baseline drift, overflow and ocular artifacts, and filtered from 1 Hz to 50 Hz to remove any residual noise. A discrete wavelet transform (DWT) was then employed to decompose the EEG signals with a 6-layer “Daubechies” wavelet and eliminate motion artifacts [24,25]. Briefly, the DWT decomposes selected EEG signals into a number of layers by filtering the signals with quadrature mirror filters (a low-pass filter and a high-pass filter). The output of each layer is then a series of detail coefficients (from the high-pass filter) and approximation coefficients (from the low-pass filter) [26]. DWT-based denoising relies on the assumption that the coefficients associated with the motion artifacts yield much smaller values than those of true EEG signal. With this in mind, the cleaned EEG signals can be reconstructed by setting an appropriate threshold and eliminating these coefficients. After denoising, the EEG signals from all channels were re-referenced by subtracting the average signal from two EEG channels placed on the binaural mastoids. Single-trial EEG signals within each task period (0–5-s; 5000 data points) were then segmented with respect to different grid levels.

2.5. Multi-scale permutation transfer entropy

Transfer entropy (TE) is a widely used directional information measurement method that generally explains the causality of time series based on information theory [27].

Briefly, let $X = \{x_1, x_2, \dots, x_n\}$ and $Y = \{y_1, y_2, \dots, y_n\}$ be two time series, each with a length of n . The TE from Y to X is defined as:

$$T_{Y \rightarrow X} = \sum_{x_t, y_t} p(x_t, x_{t-1}^{t-p}, y_{t-1}^{t-p}) \log \frac{p(x_t | x_{t-1}^{t-p}, y_{t-1}^{t-p})}{p(x_t | x_{t-1}^{t-p})} \tag{1}$$

where $x_{t-1}^{t-p}, y_{t-1}^{t-p}$ represents the vector variable describing all the states visited by X and Y between time $t-1$ and time $t-p$. $p(a)$ represents the probability associated with the vector variable a , and $p(b|a)$ represents the probability of the scalar variable b conditioned to a .

The multi-scale permutation transfer entropy (MPTE) is an advanced form of TE. Briefly, to compute the MPTE of a given time series signal X , the signal is first symbolized with multiple scales, which is given as:

$$X^S = \begin{cases} S-1 & , & x_i \geq X_{S-1} \\ \vdots & & \vdots \\ 1 & , & X_2 > x_i \geq X_1 \\ 0 & , & x_i < X_1 \end{cases} \tag{2}$$

where S is the scale, representing the number of symbols, and x_i is an element of the original data. The larger the S value, the closer the symbol sequence is to the original sequence. However, if S is too large, it will exaggerate the influence of noise, reducing robustness and increasing the computation complexity. Fig. 3 shows an original EEG

Table 1
Demographic information of the subjects.

Subject	Age	Used hand	Month post stroke	Condition
S1	45	right	2	Right limbs mild paralysis
S2	47	right	1	Right limbs mild paralysis
S3	49	right	1	Right upper limbs mild paralysis
S4	51	right	2	Right upper limbs mild paralysis
S5	48	right	1	Right limbs mild paralysis

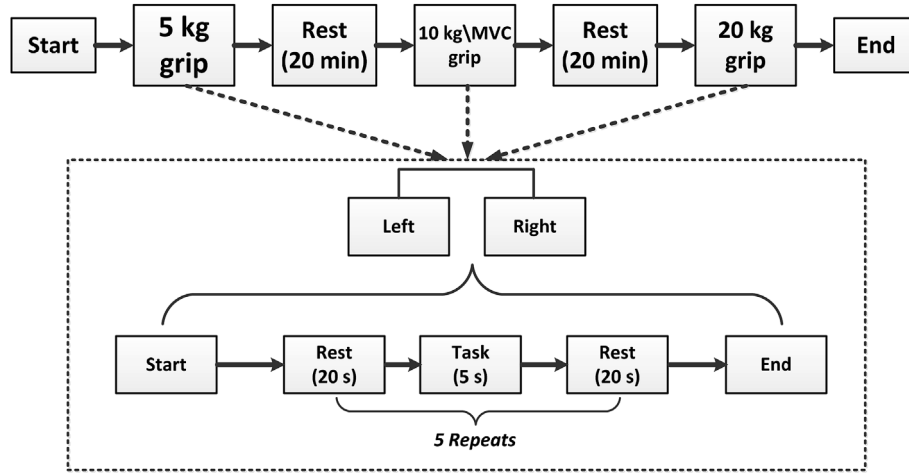


Fig. 1. Illustration of the experimental paradigm. The patient group performed MVC using only their affected hand.

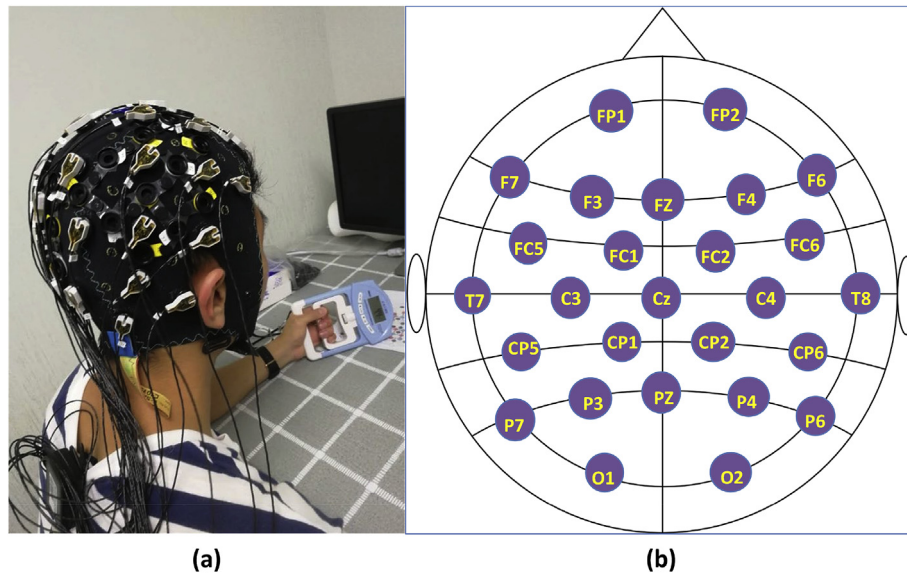


Fig. 2. (a) Experimental environment of the EEG data collection; (b) Illustration of the locations of EEG electrodes.

signal from a patient and the corresponding signals symbolized with different scales.

After the symbolization of X , the phase space of X is reconstructed by (3):

$$X_t^S = \{x_t^s, x_{t+\tau}^s, \dots, x_{t+(m-1)\tau}^s\} \quad (3)$$

where m is the embedded dimension, τ is time delay, X_t^S is the t -th space vector, and x_t^s is the element of the space vector X_t^S .

Generally, selecting a large embedding dimension m is likely to degrade the temporal characteristics of the signal. Bandt suggests that an appropriate embedding dimension m ranges from 3 to 7 [12], and evidence suggests that m should be set to 3 for severely non-stationary EEG signals [23,24]. An extremely large or small delay time τ may also reduce the correlation of the vector in the phase space or retain a large number of redundant information within the signal. Consequently, τ was set to 1 in this study.

After constructing the phase space, the probability distribution of the permutation patterns was estimated. Each space vector corresponds to a type of permutation and each permutation corresponds to multiple space vectors, such that there exist $m!$ possible permutations of the space vectors. Let the number of space vectors for each permutation be denoted by M_j ($j=1,2,3 \dots, m!$). The probability associated with the permutation (M_j) at the scale S is then given as:

$$P_{M_j}^S = \frac{M_j}{n - m + 1} \quad (4)$$

where n is the length of the original data, m is the embedded dimension, and $n - m + 1$ is the number of the space vectors.

Finally, the MPTE of the signal in scale p can be obtained by using equation (4) to define the probabilities in equation (1). More details regarding the MPTE and its calculation can be found in Ref. [28]. For each subject, the MPTE at each grid level was calculated as the mean MPTE of all five repeated trials.

2.6. Coupling analysis of EEG signals based on MPTE

In order to study the coupling properties between different EEG channels at different frequency bands, the preprocessed and segmented EEG signals were divided into 49 sub-bands, each with bandwidth of 1Hz, and the MPTE values of these sub-bands were calculated at different scales. Based on the contralateral control theory of the brain [29], the coupling relationships between the C3 channel (the left motor area) and the CP5 channel (left sensory area) were analyzed during the right hand grip task. Similarly, the coupling relationships between the C4 channel (right motor area) and the CP6 channel (right sensory area) were analyzed during the left hand grip task.

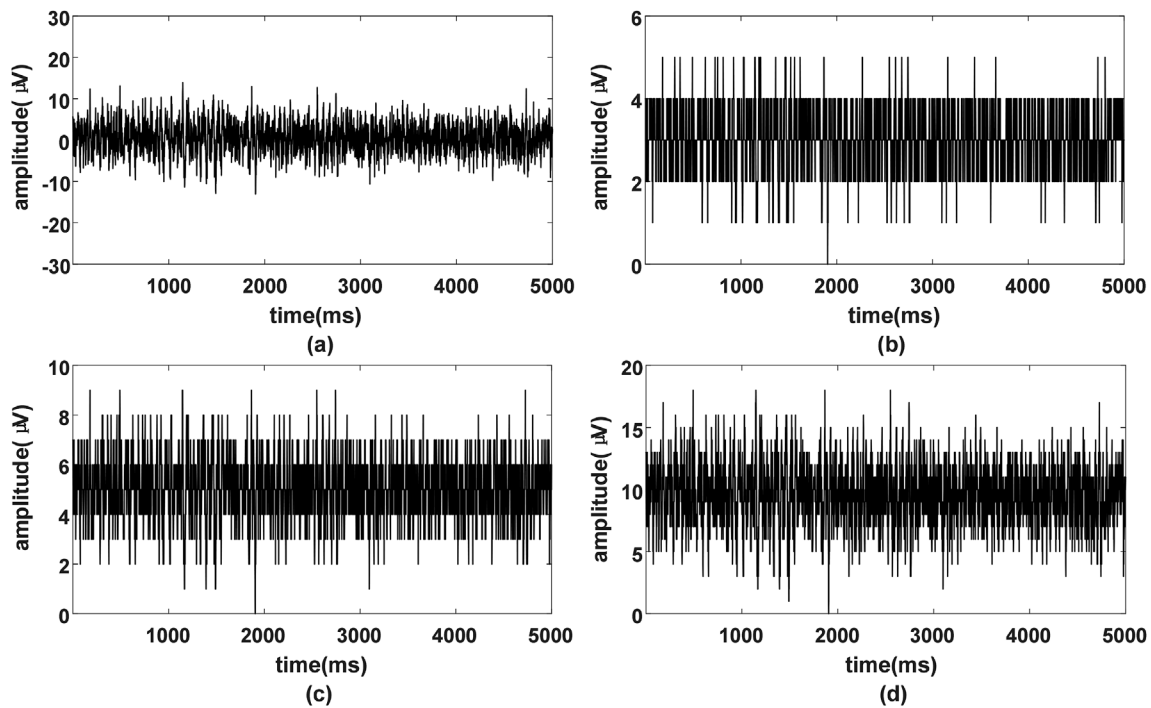


Fig. 3. One original EEG signal (a) at C3 channel of a patient subject and its corresponding signals symbolized at scale #5 (b), scale #9 (c), and scale #18 (d).

The coupling degree of EEG signals can be quantitatively assessed as the significant indicator of the MPTE [30]. This significant indicator, A_p , at the scale of p , is defined as:

$$A_p = \sum_f \Delta f * MPTE_p(f) \quad (5)$$

where Δf represents frequency resolution, and $MPTE_p(f)$ represents the MPTE at f band and p scale. The greater the A_p , the stronger the coupling of the EEG signals.

3. Results

3.1. The coupling analysis in multiple frequency bands and scales

The coupling strength (A_p) between EEG signals at each frequency band (theta band: 4–8 Hz, alpha band: 8–14 Hz, beta band: 15–35 Hz, gamma band: 35–50 Hz) was computed by summing the coupling strengths of all 1-Hz sub-bands at different scales for the six healthy controls (S6–S11). Fig. 4 shows the group-average coupling strength between the motor area (C4) and the sensory area (CP6) of the right hemisphere during the left hand grip task, while Fig. 5 shows the average coupling strength between the motor area (C3) and the sensory area (CP5) of the left hemisphere during the right hand grip task for healthy controls. Results suggest that a bi-directional coupling relationship exists between the contralateral brain regions – the coupling strength in the left hemisphere during right grip task tended to be stronger in both directions. Results also indicate that the coupling strengths between motor and sensory areas, regardless of the direction, were higher in the beta and gamma bands when performing lower grip force tasks.

Interestingly, for all grip tasks, the beta band consistently exhibited stronger coupling strength across all scales, as demonstrated in Figs. 4 and 5. In particular, the coupling strength in each frequency band became stronger as the scale increased. Previous studies have suggested that lower scaling generally caused a drastic reduction in the detail and dynamic information available in signals, while higher scaling might aggravate the effects of noise, reducing the robustness of the algorithm and increasing the complexity of the algorithm [31,32]. Therefore, the

scale selection is of great import for coupling analysis – scaling factors must be chosen at a level that maintains sufficient signal detail while ensuring the high robustness and low computational complexity of the algorithm. Based on experimental results, a scaling value of 18 was found to be appropriate for the analysis performed in this study.

We further investigated the coupling strengths between the motor and sensory areas during the left and right hand grip tasks in the beta band, which exhibited the greatest coupling strength of all frequency bands (Figs. 4 and 5). Coupling results for all healthy controls are summarized in Fig. 6. It can be observed that, when compared to the left hand, right hand gripping tasks showed significantly increased coupling strength between the motor area and the sensory area ($p < 0.05$). The coupling strength was also seen to decrease as the grip strength increased.

3.2. Analysis of the coupling in healthy and stroke groups

Comparisons between the beta-band coupling strength of the motor and sensory areas for all healthy controls and stroke patients are shown in Fig. 7. As stroke patients were unable to perform grip task at or over the 10 kg level using their affected hands, EEG signals were only collected and analyzed for the 5 kg and MVC conditions on affected side. The mean MVC across all patients was nearly 10 kg (9.2 ± 1.1 kg).

Overall, the coupling strength between the motor and sensory areas of each hemisphere was significantly greater in healthy group ($p < 0.05$), as shown in the Fig. 7. This indicates that the coupling between the motor area and the sensory area of healthy brains was stronger than the coupling in stroke-affected brains during active motor tasks. Statistical results are summarized in Table 2.

4. Discussion

Permutation mutual information, a measure of the coherence between signals, can be used to enhance the accuracy of probability estimation when calculating the entropy of a signal. Unfortunately, it is unable to characterize the direction of the information flow between brain regions. In contrast to permutation mutual information, TE and its enhanced forms are model-free implementations of causality analysis

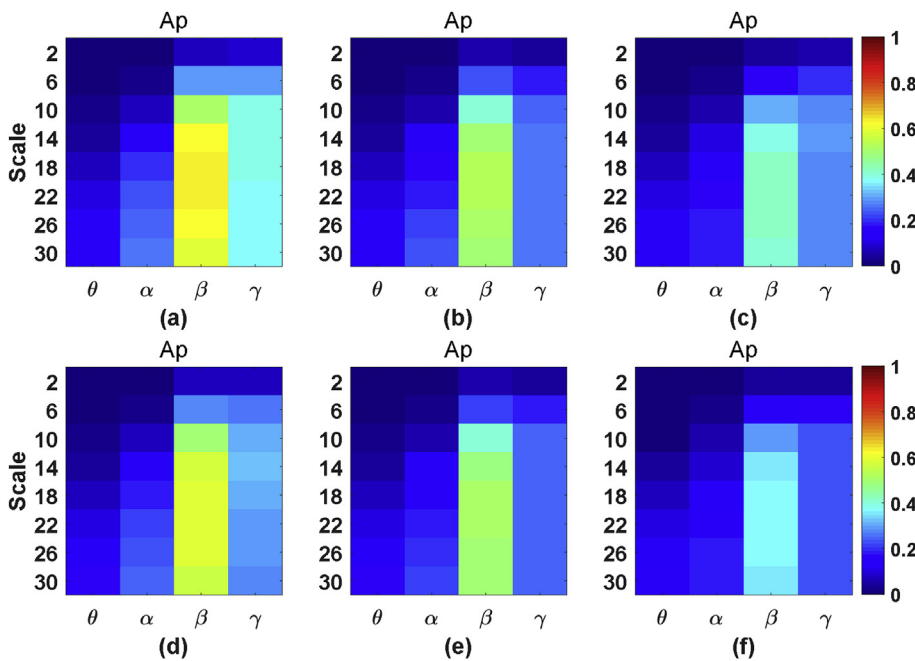


Fig. 4. The average coupling strength (A_p) between the motor area and sensory area at right hemisphere during left hand grip tasks for the healthy group. (a) 5 kg, motor area -> sensory area; (b) 10 kg, motor area -> sensory area; (c) 20 kg, motor area -> sensory area; (d) 5 kg, sensory area -> motor area; (e) 10 kg, sensory area -> motor area; (f) 20 kg, sensory area -> motor area.

that have been widely used to characterize directional flow of information between brain regions. TE methods are generally limited by the need for a large quantity of EEG data, however, making it difficult to precisely capture the coupling properties of EEG signals. The proposed MPTE approach is an enhanced method that combines permutation mutual information and TE to overcome this limitation in the coupling analysis of EEG. In this study, the MPTE was introduced and employed to assess the coupling of specific regions during motor tasks, providing a promising approach to study task-based coupling between multiple brain regions.

The oscillatory EEG activity is typically observed during the execution of steady-state isometric contractions and phasic movements. Further, it is frequently coupled with muscle activation across several different frequency bands, depending on the functions and tasks engaged within the motor system. According to previous studies, beta-

band oscillations are primarily associated with mild to moderate isometric contraction [33,34]. This is in line with current MPTE results, which consistently identified strong bi-directional beta-band coupling between the motor area and sensory area during hand gripping tasks, as shown in Figs. 4 and 5. In particular, this coupling pattern was reliably observed in both healthy controls and patients group (Fig. 7), indicating the important role that the beta band plays in the execution and control of movement. It is also noteworthy that, as grip strength increased, coupling strength showed a corresponding decrease, and that the coupling strength of the contralateral motor area and sensory area was more prominent during the right hand grip task for all healthy controls (Fig. 6). According to the theory of the contralateral motor control, the left hemisphere would be heavily implicated in the dominant-hand movement of a right-handed person, which should be more exercised and developed than the non-dominant hand [35,36]. This aligns with

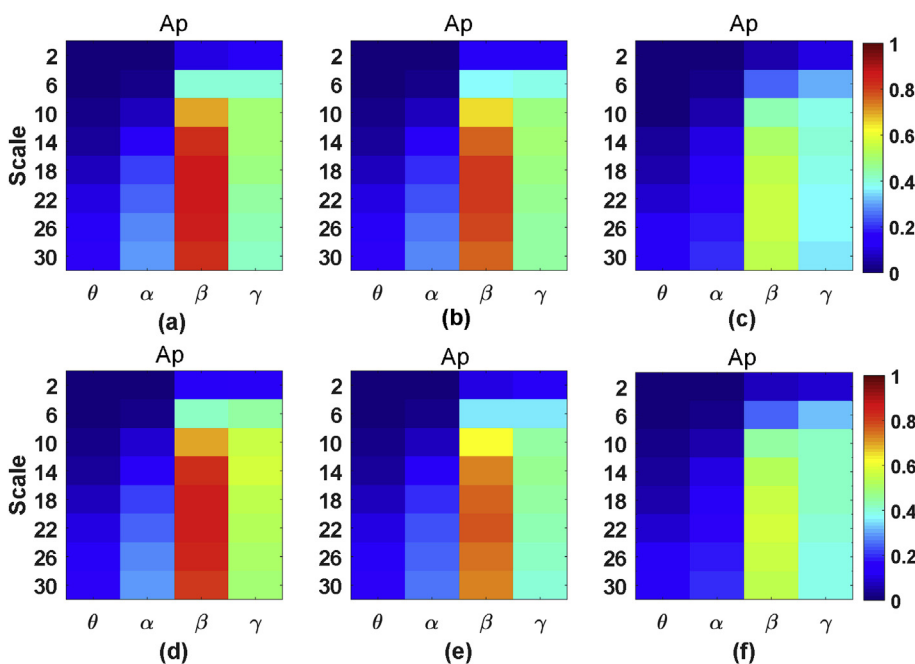


Fig. 5. The average coupling strength (A_p) between the motor area and sensory area of the left hemisphere during right hand grip tasks for healthy group. (a) 5 kg, motor area -> sensory area; (b) 10 kg, motor area -> sensory area; (c) 20 kg, motor area -> sensory area; (d) 5 kg, sensory area -> motor area; (e) 10 kg, sensory area -> motor area; (f) 20 kg, sensory area -> motor area.

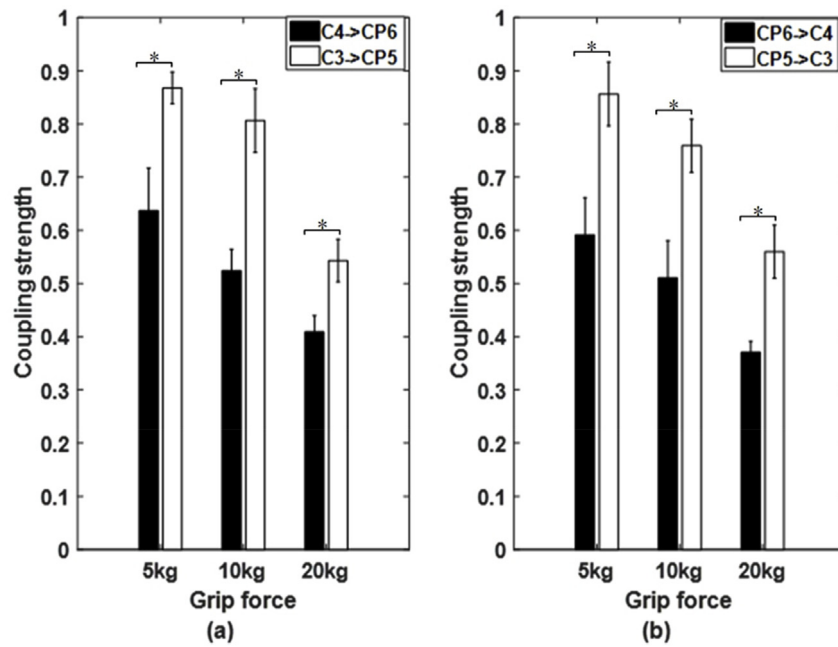


Fig. 6. Comparison of bi-directional coupling strength at beta band in healthy group during hand grip task. (a) motor area -> sensory area (b) sensory area -> motor area. The “*” indicates a significant difference ($p < 0.05$).

the obtained experimental results, as healthy controls were all right-handed in this study. Therefore, the present findings are not only valuable supplements to the previous studies, but also provide new insight into cortical interactions and the control of willed motion.

Although the coupling strength between the motor area and sensory area was consistently stronger in beta band for both groups, stroke patients exhibited noticeably weaker inter-regional coupling during all motor tasks. Significant group differences were found between stroke patients and healthy controls when performing the 5 kg grip task with

either hand (Fig. 7 and Table 2). One potential explanation is that stroke disrupts patients’ motor or sensory areas in both hemispheres, reducing the connection between them. With this in mind, our findings may serve as a routine approach for the assessment and monitoring of motor dysfunction in future clinical applications.

Results demonstrate that the proposed MPTE method holds great promise as an advanced approach to characterize the coupling of multiple brain regions across multiple bands and multiple scales, providing a theoretical basis for exploring the rehabilitation of human

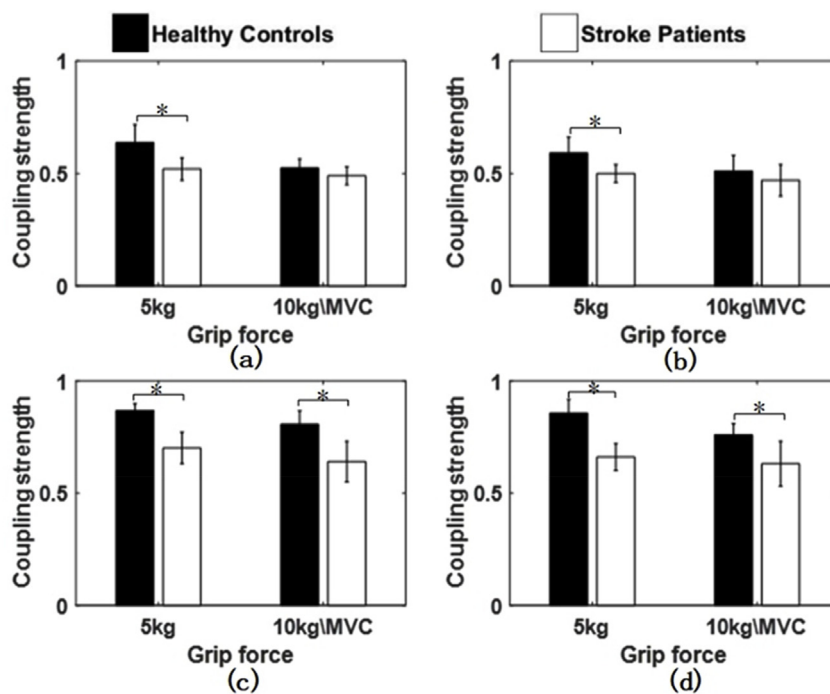


Fig. 7. Comparison of the coupling strength in healthy and stroke groups during left and right grip tasks. (a) Left hand, motor area -> sensory area; (b) Left hand, sensory area -> motor area; (c) Right hand, motor area -> sensory area; (d) Right hand, sensory area -> motor area. The “*” indicates a significant difference ($p < 0.05$).

Table 2The statistical analysis result of the coupling strengths (A_p) between healthy controls (HC) and stroke patients (SP).

	Left hand				Right hand			
	C4- > CP6		CP6- > C4		C3- > CP5		CP5- > C3	
	5 kg	10 kg\MVC						
HC	0.64 ± 0.08	0.52 ± 0.04	0.59 ± 0.07	0.51 ± 0.07	0.87 ± 0.03	0.81 ± 0.06	0.86 ± 0.06	0.76 ± 0.05
SP	0.52 ± 0.05	0.49 ± 0.04	0.50 ± 0.04	0.47 ± 0.07	0.70 ± 0.07	0.64 ± 0.09	0.66 ± 0.06	0.63 ± 0.10
<i>p</i>	0.03	0.15	0.025	0.43	0.02	0.01	0.01	0.04

motor system control. It should be recognized, however, that the limited sample size of this study makes it difficult to draw concrete conclusions regarding the clinical value of the MPTE, although clear patterns and differences between healthy controls and patients were presented. It is expected that in future work will recruit a larger subject population to enable advanced analysis and validate the present findings, potentially fitting regression models between the MPTE and corresponding clinical rating scores, or employing advanced classification techniques to identify motor function-related biomarkers for the assessment of rehabilitation after stroke. In addition, the selection of an appropriate scale for analysis should be carefully considered. In the present study a scale of 18 was selected as an appropriate scale by direct observation, although the distribution pattern of the coupling strengths in the selected frequency bands tended to be consistent across scales (Figs. 4 and 5). Further efforts should be taken to explore this topic and improve the efficacy of the MPTE method in future work.

5. Conclusion

The coupling of EEG signals reflects the interaction between brain regions, including interaction strength and direction, and is therefore of great importance for the assessment of motor function in post-stroke patients. In this study the MPTE measure was introduced and employed to characterize the directional coupling between sensory and motor areas for both healthy and patient subjects. Result revealed that coupling strength between the motor area and the sensory area was weaker in beta band of stroke patients, as compared to healthy controls. Although a larger sample size is needed to validate the current finding, the present study suggests the potential of the MPTE as an approach for studying the mechanism of functional motor deficits and recovery in stroke patients.

Disclosures

The authors declare that there is no conflict of interest regarding the publication of this article.

Acknowledgements

Project supported by the Natural Science Foundation of China (Grant No.61871427), Zhejiang Natural Science Foundation (Grant No. LY18F030009), Research Innovation Foundation of Hangzhou Dianzi University (Grant No. CXJJ2018089), and the University of Houston. The authors would like to thank Thomas Potter from the University of Houston, for proofreading and polishing the manuscript.

References

- [1] S.Y. Kim, W. Lim, Emergence of ultrafast sparsely synchronized rhythms and their responses to external stimuli in an inhomogeneous small-world complex neuronal network, *Neural Network*. 93 (2017) 57–75, <https://doi.org/10.1016/j.neunet.2017.04.002>.
- [2] V.N. Murthy, E.E. Fetz, Coherent 25-hz to 35-hz oscillations in the sensorimotor cortex of awake behaving monkeys, *P Natl Acad Sci USA* 89 (1992) 5670–5674, <https://doi.org/10.1073/pnas.89.12.5670>.
- [3] D. Wen, Y.H. Zhou, X.L. Li, A critical review: coupling and synchronization analysis methods of EEG signal with mild cognitive impairment, *Front. Aging Neurosci.* 7 (2015), <https://doi.org/10.3389/fnagi.2015.00054>.
- [4] M. Borowska, E. Oczeretko, P. Sobaniec, W. Sobaniec, Nonlinear Synchronization Analysis of the EEG Signals 31 6th World Congress of BiomechanicsWcb, 2010, p. 1362, https://doi.org/10.1007/978-3-642-14515-5_347 2010.
- [5] P.J. Uhlhaas, F. Roux, E. Rodriguez, A. Rotarska-Jagiela, W. Singer, Neural synchrony and the development of cortical networks, *Trends Cognit. Sci.* 14 (2010) 72–80, <https://doi.org/10.1016/j.tics.2009.12.002>.
- [6] C.J. Stam, Nonlinear dynamical analysis of EEG and MEG: review of an emerging field, *Clin. Neurophysiol.* 116 (2005) 2266–2301, <https://doi.org/10.1016/j.clinph.2005.06.011>.
- [7] J.L. Zhang, M.Y. Zhang, N. Jiang, Age-related phase synchronization analysis of alpha rhythm for normal EEG signals, *J Med Imag Health In* 7 (2017) 1–6, <https://doi.org/10.1166/jmihi.2017.1978>.
- [8] C. Guerrero-Mosquera, M. Verleysen, A.N. Vazquez, EEG feature selection using mutual information and support vector machine: a comparative analysis, Annual International Conference of the IEEE Engineering in Medicine and Biology Society, EMBC, 2010, pp. 4946–4949, <https://doi.org/10.1109/IEMBS.2010.5627239> 2010.
- [9] L. Tomasevic, G. Zito, P. Pasqualetti, M.M. Filippi, D. Landi, A. Ghazaryan, D. Lupoi, C. Porcaro, F. Bagnato, P.M. Rossini, F. Tecchio, Cortico-muscular coherence as an index of fatigue in multiple sclerosis, *Mult. Scler. J* 19 (2013) 334–343, <https://doi.org/10.1177/1352458512452921>.
- [10] H. Kanazawa, M. Kawai, T. Kinai, K. Iwanaga, T. Mima, T. Heike, Cortical muscle control of spontaneous movements in human neonates, *Eur. J. Neurosci.* 40 (2014) 2548–2553, <https://doi.org/10.1111/ejn.12612>.
- [11] J. Li, J.Q. Yan, X.Z. Liu, G.X. Ouyang, Using permutation entropy to measure the changes in EEG signals during absence seizures, *Entropy-Switz* 16 (2014) 3049–3061, <https://doi.org/10.3390/e16063049>.
- [12] C. Bandt, B. Pompe, Permutation entropy: a natural complexity measure for time series, *Phys. Rev. Lett.* 88 (2002), <https://doi.org/10.1103/PhysRevLett.88.174102>.
- [13] F.C. Morabito, D. Labate, F. La Foresta, A. Bramanti, G. Morabito, I. Palamara, Multivariate multi-scale permutation entropy for complexity analysis of alzheimer's disease EEG, *Entropy-Switz* 14 (2012) 1186–1202, <https://doi.org/10.3390/e14071186>.
- [14] E. Sitnikova, T. Dikanov, D. Smirnov, B. Bezruchko, G. Van Luijtelara, Granger causality: cortico-thalamic interdependencies during absence seizures in WAG/Rij rats, *J. Neurosci. Methods* 170 (2008) 245–254, <https://doi.org/10.1016/j.jneumeth.2008.01.017>.
- [15] M.H.I. Shovon, N. Nandagopal, R. Vijayalakshmi, J.T. Du, B. Cocks, Directed connectivity analysis of functional brain networks during cognitive activity using transfer entropy, *Neural Process. Lett.* 45 (2017) 807–824, <https://doi.org/10.1007/s11063-016-9506-1>.
- [16] B. Schelter, J. Timmer, M. Eichler, Assessing the strength of directed influences among neural signals using renormalized partial directed coherence, *J. Neurosci. Methods* 179 (2009) 121–130, <https://doi.org/10.1016/j.jneumeth.2009.01.006>.
- [17] A.K. Seth, A MATLAB toolbox for Granger causal connectivity analysis, *J. Neurosci. Methods* 186 (2010) 262–273, <https://doi.org/10.1016/j.jneumeth.2009.11.020>.
- [18] M. Costa, A.L. Goldberger, C.K. Peng, Multiscale entropy analysis of complex physiologic time series, *Phys. Rev. Lett.* 89 (2002), <https://doi.org/10.1103/PhysRevLett.89.068102>.
- [19] X. Li, X.Y. Qi, X.Q. Sun, J.L. Xie, M.D. Fan, J.N. Kang, An improved multi-scale entropy algorithm in emotion EEG features extraction, *J Med Imag Health In* 7 (2017) 436–439, <https://doi.org/10.1166/jmihi.2017.2031>.
- [20] A. Bhattacharyya, R.B. Pachori, A. Upadhyay, U.R. Acharya, Tunable-QWavelet transform based multiscale entropy measure for automated classification of epileptic EEG signals, *Appl Sci-Basel* 7 (2017), <https://doi.org/10.3390/app7040385>.
- [21] M. Staniek, K. Lehnertz, Symbolic transfer entropy, *Phys. Rev. Lett.* 100 (2008), <https://doi.org/10.1103/PhysRevLett.100.158101>.
- [22] J. Lee, S. Nemati, I. Silva, B.A. Edwards, J.P. Butler, A. Malhotra, Transfer entropy estimation and directional coupling change detection in biomedical time series, *Biomed. Eng. Online* 11 (2012), <https://doi.org/10.1186/1475-925x-11-19>.
- [23] K. Hlavackova-Schindler, M. Palus, M. Vejmelka, J. Bhattacharya, Causality detection based on information-theoretic approaches in time series analysis, *Phys. Rep.* 441 (2007) 1–46, <https://doi.org/10.1016/j.physrep.2006.12.004>.
- [24] A. Khare, U.S. Tiwary, W. Pedrycz, M. Jeon, Multilevel adaptive thresholding and

- shrinkage technique for denoising using Daubechies complex wavelet transform, *Imaging Sci. J.* 58 (2010) 340–358, <https://doi.org/10.1179/136821910x12750339175826>.
- [25] C. Chen, N.N. Zhou, A New Wavelet Hard Threshold to Process Image with Strong Gaussian Noise, *IEEE Fifth International Conference on Advanced Computational Intelligence (ICACI)*, 2012, pp. 558–561 2012.
- [26] R.H. Li, T. Potter, W.T. Huang, Y.C. Zhang, Enhancing performance of a hybrid EEG-fnirs system using channel selection and early temporal features, *Front. Hum. Neurosci.* (2017) 11, <https://doi.org/10.3339/Fnhum.2017.00462>.
- [27] F.P. Santos, C.D. Maciel, P.L. Newland, Pre-processing and transfer entropy measures in motor neurons controlling limb movements, *J. Comput. Neurosci.* 43 (2017) 159–171, <https://doi.org/10.1007/s10827-017-0656-6>.
- [28] W.P. Yao, J. Wang, Multi-scale symbolic transfer entropy analysis of EEG, *Physica A* 484 (2017) 276–281, <https://doi.org/10.1016/j.physa.2017.04.181>.
- [29] L.J. Carr, L.M. Harrison, A.L. Evans, J.A. Stephens, Patterns of central motor re-organization in hemiplegic cerebral-palsy, *Brain* 116 (1993) 1223–1247, <https://doi.org/10.1093/brain/116.5.1223>.
- [30] P. Ma, Y. Chen, Y. Du, Y. Su, X. Wu, Z. Liang, P. Xie, Analysis of corticomuscular coherence during rehabilitation exercises after stroke, *Sheng Wu Yi Xue Gong Cheng Xue Za Zhi* 31 (2014) 971–977.
- [31] D. Lind, B. Marcus, *An Introduction to Symbolic Dynamics and Coding*, Cambridge university press, 1995.
- [32] E.A. Jackson, *Perspectives of Nonlinear Dynamics*, CUP Archive1992.
- [33] E. Lattari, B. Velasques, M. Cunha, H. Budde, L. Basile, M. Cagy, R. Piedade, S. Machado, P. Ribeiro, Corticomuscular coherence behavior in fine motor control of force: a critical review, *Rev. Neurol.* 51 (2010) 610–623.
- [34] T. Gilbertson, E. Lalo, L. Doyle, V. Di Lazzaro, B. Cioni, P. Brown, Existing motor state is favored at the expense of new movement during 13-35 Hz oscillatory synchrony in the human corticospinal system, *J. Neurosci.* 25 (2005) 7771–7779, <https://doi.org/10.1523/Jneurosci.1762-05.2005>.
- [35] G.K. York, D.A. Steinberg, Contralateral control, *Neurology* 45 (1995), <https://doi.org/10.1212/Wnl.45.12.2297> 2297–2297.
- [36] D.P. Carey, E.L. Hargreaves, M.A. Goodale, Reaching to ipsilateral or contralateral targets: within-hemisphere visuomotor processing cannot explain hemispatial differences in motor control, *Exp. Brain Res.* 112 (1996) 496–504, <https://doi.org/10.1007/BF00227955>.